ELSEVIER

Fluid Phase Equilibria 213 (2003) 19–37

FLUID PHASE EQUILIBRIA

www.elsevier.com/locate/fluid

Alternate equation of state combining rules and interaction parameter generalizations for asymmetric mixtures

Wuzi Gao, Robert L. Robinson Jr., Khaled A.M. Gasem*

School of Chemical Engineering, Oklahoma State University, Engineering North 423, Stillwater, OK 74078-0537, USA

Received 18 June 2002; accepted 10 March 2003

Abstract

Following the work of Juris and Wenzel, an alternate combining rule is proposed for cubic equations of state (CEOS). A wide variety of interactions between unlike molecules can be represented effectively by this combining rule.

The Soave–Redlich–Kwong (SRK) and Peng–Robinson (PR) equations of state (EOS) have been used to assess the usefulness of the alternate combining rule in describing the types of unlike interactions encountered in asymmetric mixtures. In addition, a study was undertaken to evaluate the predictive capability of both equations of state in representing vapor–liquid equilibrium (VLE) of asymmetric binary mixtures, involving methane, ethane, nitrogen, hydrogen, carbon monoxide and carbon dioxide in *n*-paraffins (C_4–C_{44}).

EOS binary interaction parameters generated by the proposed combination rules are presented for the systems considered. The quality of the EOS representation is dependent on the level of complexity applied in the parameter regressions. Overall, average absolute deviations of 1–3% are realized from the various regression scenarios. In addition, generalized EOS parameter correlations for system-dependent parameters have been developed. These generalized interaction parameters represent the solubilities of the selected systems within 5%.

Keywords: Equation of state (EOS); Combining rules; Interaction parameters; Peng–Robinson EOS; Soave EOS; Parameter generalization; Asymmetric mixtures; Supercritical fluids

1. Introduction

Precise descriptions of fluid-phase behavior can have significant economic impact when used in chemical engineering process calculations, such as phase separations. These descriptions must be undertaken in terms of analytical models suited for process design/development calculations. Almost all state-of-the-art analytical models, such as EOS or activity coefficient models, have one or more empirical "interaction" parameters for precise model tuning [4]. Although these parameters cannot be predicted a priori from theory

* Corresponding author. Tel.: +1-405-744-5280; fax: +1-405-744-6338.
E-mail address: gasem@okstate.edu (K.A.M. Gasem).

0378-3812/$ – see front matter © 2003 Elsevier B.V. All rights reserved.
doi:10.1016/S0378-3812(03)00123-7

at present, they can have dramatic effects on phase behavior calculations. Typically, interaction parameters are regressed from the available experimental data, and provisions are made, through parameter generalizations, to estimate them for systems lacking experimental data. Accurate parameter generalizations are necessary since it is infeasible to conduct enough experiments to cover all binaries and all phase conditions.

Asymmetric mixtures involving light gas solutes (hydrogen, nitrogen, CO, CO_2, methane, and ethane) and hydrocarbon solvents (*n*-paraffins C_4–C_{44}) are encountered in many important industries, such as enhanced oil recovery, supercritical extraction, and Fisher–Tropsch syntheses. In this study, cubic equations of state (CEOS) have been chosen to describe the equilibrium properties of such systems. Although these simple CEOS are not as rigorous as theoretically-based equations of state (EOS), such as the simplified-perturbed-hard-chain theory (SPHCT) EOS [5,6], the simplified-statistical-associating-fluid theory (SAFT) EOS [7] and the modified Park–Gasem–Robinson (MPGR) EOS [8], their simplicity, relative accuracy and wide industrial use justify their further development [4].

Proper mixing rules are required to extend EOS applications to mixtures. As a result, numerous mixing rules have been developed and evaluated (see e.g. [9–13]). Nevertheless, the one-fluid theory mixing rules are found to be both simple and, in most cases, accurate. In many applications, CEOS with these mixing rules can be used to represent the systems within the experimental precision [10]. Often, one interaction parameter is sufficient for the purpose. Also, the interaction parameters from these mixing rules show regular trends with solvent size, when dealing with a particular homologous series. Although many other mixing rules, such as Wong–Sandler mixing rules [12], are more theoretically based and can be used to represent asymmetric mixtures precisely [14], the multiple parameters associated with these mixing rules complicate developing simple parameter generalizations. Therefore, we have elected to use the classical one-fluid quadratic mixing rules.

Embedded in mixing rules are combining rules to account for the unlike molecular interactions. Interestingly, while the literature reflects a great interest in mixing rules, there are fewer studies of combining rules, especially those pertaining to CEOS. Historically, the use of a geometric-mean combining rule for the attraction law constant '*a*' and a linear combining rule for the co-volume '*b*' is most common when dealing with CEOS. In contrast, a variety of combining rules has been developed for virial-type EOS (see e.g. [1,15]). In the present work, we apply a general form of a combining rule suggested for use in virial-type EOS by Juris and Wenzel [1].

Once a set of mixing and combining rules was selected, binary interaction parameters were regressed from available data to represent precisely the mixture vapor–liquid equilibrium (VLE) properties. Moreover, attempts were made to generalize these parameters for systems and phase conditions not accounted for in the existing experimental database. Literature generalizations have been reviewed by several investigators (see e.g. [16–18]). Our previous parameter generalizations involving asymmetric mixtures have varied in complexity (e.g. [4,19,20]). In this study, we present new generalized correlations for EOS binary interaction parameters, which benefit from (a) an expanded binary mixture database, (b) more accurate heavy *n*-paraffin pure fluid properties, and (c) an alternate EOS combining rule.

2. Equations of state

The SRK EOS is [2]

$$p = \frac{RT}{v-b} - \frac{a}{v(v+b)} \tag{1}$$

where

$$a = a_c \alpha(T) \tag{2}$$

$$b = \frac{0.08664 R T_c}{p_c} \tag{3}$$

and

$$a_c = \frac{0.42748 R^2 T_c^2}{p_c} \tag{4}$$

$$\alpha^{1/2} = 1 + k(1 - T_r^{1/2}) \tag{5}$$

$$k = 0.480 + 1.574\omega - 0.176\omega^2 \tag{6}$$

Similarly, the PR EOS is [3]

$$p = \frac{RT}{v - b} - \frac{a}{v(v + b) + b(v - b)} \tag{7}$$

where

$$a = a_c \alpha(T) \tag{8}$$

$$b = \frac{0.0778 R T_c}{p_c} \tag{9}$$

and

$$a_c = \frac{0.45724 R^2 T_c^2}{p_c} \tag{10}$$

$$\alpha^{1/2} = 1 + k(1 - T_r^{1/2}) \tag{11}$$

$$k = 0.37464 + 1.54226\omega - 0.26992\omega^2 \tag{12}$$

where p is the pressure, R the gas constant, T the temperature, a and b are EOS constants, v the molar volume, T_c the critical temperature, p_c the critical pressure, T_r the reduced temperature, $\alpha(T)$ expresses the temperature dependence in the parameter a, and ω the acentric factor. For the PR EOS, we also use a newly-developed α function [21]

$$\alpha = \exp[(2.00 + 0.836 T_r)(1 - T_r^{k})] \tag{13}$$

where

$$k = 0.134 + 0.508\omega - 0.467\omega^2$$

which yields more accurate vapor pressure predictions for the heavy hydrocarbons than those obtained using Eqs. (11) and (12).

3. Mixing rules

To apply the SRK and PR EOS to mixtures, mixing rules are employed to calculate the values of a and b of the mixtures. Classic, one-fluid quadratic mixing rules are employed in this study

$$a = \sum_{i}^{N}\sum_{j}^{N} z_i z_j a_{ij} \tag{14}$$

$$b = \sum_{i}^{N}\sum_{j}^{N} z_i z_j b_{ij} \tag{15}$$

where z_k represents the mole fraction of component "k" in a mixture, and N the number of components in the mixture. In Eqs. (14) and (15), the summations are over all chemical species. The cross coefficients a_{ij} and b_{ij} are parameters used in EOS calculations to reflect interactions between components "i" and "j". Typically, they are calculated from the pure-substance a and b parameters according to specified combining rules.

Different combining rules appear in the literature, especially for virial-type EOS. Some attempts have also been made to improve mixture property predictions through alternate combining rules (see e.g. [22,23]) for CEOS. Nevertheless, little improvements were realized, relative to the added complexity of the proposed rules.

Of interest in this study is the general form of the combining rule described by Juris and Wenzel [1] for the Martin–Hou EOS parameters.

$$A_{ij} = \left[\frac{A_i^{Nij} + A_j^{Nij}}{2}\right]^{1/Nij} \tag{16}$$

This combining rule is particularly interesting because it encompasses several rules used in the literature ($N \to 0$, geometric or Lorentz–Berthelot rule; $N_{ij} = 1$, linear rule; $N_{ij} = 1/3$, Lorentz rule; $N_{ij} = -1$, Halsey–Fender rule). In this work, we apply Eq. (16) in its most general form. That is, the combining rule exponent 'N' is treated as a regressed parameter; thus, the combining rule allows the experimental data for a given binary to dictate the recipe for combining the unlike molecular interactions. This treatment is similar to the approach taken by Sudibandriyo [24] to develop new mixing rules that abide by conformal solution theory. In this study, we call Eq. (16) the conformal combining rule. The efficiencies of both the traditional and conformal combining rules in representing asymmetric mixtures are evaluated in this study.

3.1. Classic (or Lorentz–Berthelot) combining rules

The classic combining rules are as follows [25]:

$$a_{ij} = (1 - C_{ij})(a_i a_j)^{1/2} \tag{17}$$

$$b_{ij} = 0.5(1 + D_{ij})(b_i + b_j) \tag{18}$$

C_{ij} and D_{ij} are empirical interaction parameters characterizing deviations from the defined (geometric or linear) unlike interactions between molecules "i" and "j". When i equals j, C_{ij} and D_{ij} are zero. When i

does not equal j, C_{ij} and D_{ij} may be non-zero. Values of C_{ij} and D_{ij} are determined by fitting experimental data to minimize a specified objective function. Eqs. (17) and (18) are equivalent to Eq. (16), when the exponent in Eq. (16) is set to an infinitely small value and 1, respectively.

3.2. Conformal combining rules

For asymmetric mixtures, the interaction between two unlike molecules can be significantly different from that represented by the geometric-mean combining rule, $a = (a_i a_j)^{1/2}$. In such cases, the binary interaction parameter used to correct for deviations from the geometric-mean can require very large values (>50% correction, i.e. $C_{ij} > 0.5$). Clearly, in such instances, a different combining rule may be more appropriate.

In this study, we adopt the following combining rules:

$$a_{ij} = \left[\frac{a_i^{N_{ij}} + a_j^{N_{ij}}}{2}\right]^{1/N_{ij}} \tag{19}$$

$$b_{ij} = \left[\frac{b_i^{M_{ij}} + b_j^{M_{ij}}}{2}\right]^{1/M_{ij}} \tag{20}$$

where the exponents N_{ij} and M_{ij} are regressed directly from the binary experimental data. In principle, these exponents should more precisely reflect the type of unlike-pair interactions than the binary interaction parameters C_{ij} and D_{ij}. That is, these combining rules elucidate the types of unlike molecular interactions, as opposed to using a corrected geometric or linear rule.

A direct connection exists between C_{ij} and N_{ij}, D_{ij} and M_{ij}, as shown below

$$C_{ij} = 1 - \left[\frac{(a_i/a_j)^{N_{ij}/2} + (a_j/a_i)^{N_{ij}/2}}{2}\right]^{1/N_{ij}} \tag{21}$$

$$D_{ij} = 1 - \frac{2}{b_i + b_j}\left[\frac{b_i^{M_{ij}} + b_j^{M_{ij}}}{2}\right]^{1/M_{ij}} \tag{22}$$

This means the quality of the EOS representation obtained from the traditional combining rules and the conformal rules are identical at a given temperature, and one set of parameters can be generated from the other. As such, use of the conformal combining rules is predicated on their ability to provide clear understanding for the *type* of molecular combinations encountered (e.g. linear, Lorentz, etc.), as opposed to accepting preset rules. In addition, the regressed exponents (N_{ij} and M_{ij}) may be easier to generalize than C_{ij} and D_{ij} for some systems, as suggested by the variation of C_{ij} with (a_j/a_i) ratio for various N_{ij} values depicted in Fig. 1.

4. Database and data reduction procedures

Table 1 presents the pure-fluid physical properties used in this study. The property values for the light components originate from Reid et al. [26], and the updated ABC model was used to predict the physical

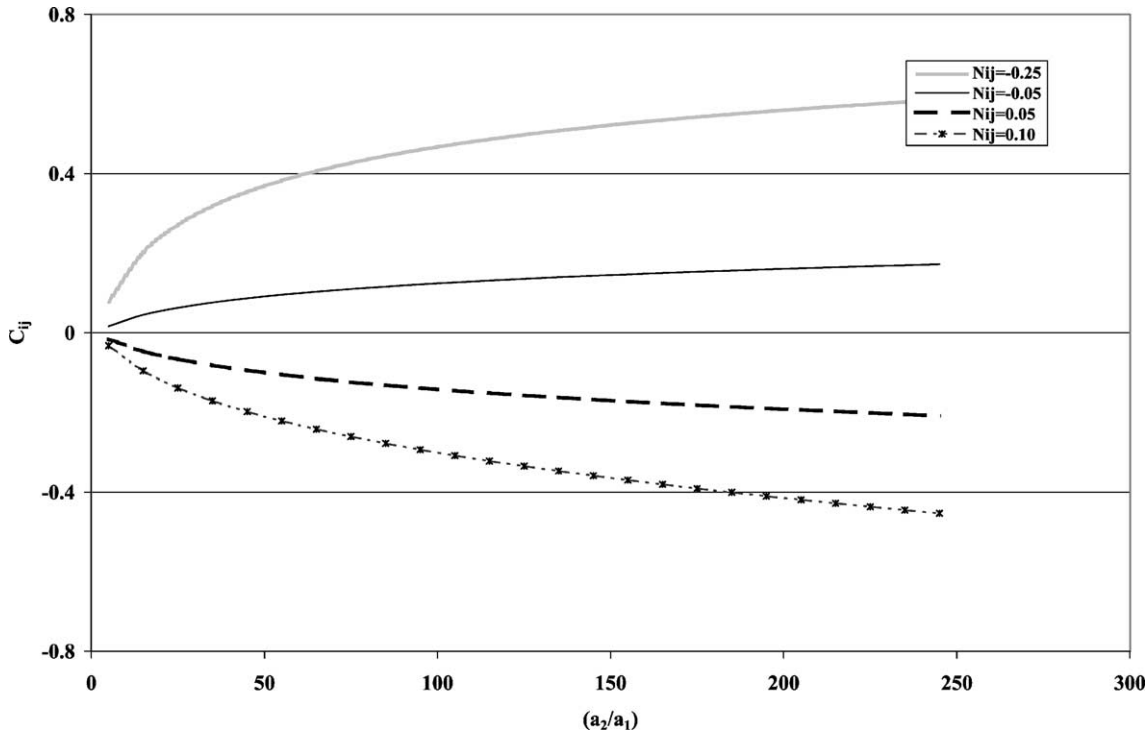

Fig. 1. The relationship between C_{ij} and (a_2/a_1) at constant N_{ij}.

properties of heavy *n*-paraffins (CN $\geq$ 10), as given by Gao et al. [27]. Table 2 details the sources of binary experimental data used in our evaluations, along with the temperature, pressure and composition range for each binary system. All data were utilized as isothermal $p - x$ measurements, i.e. the bubble point pressure as a function of solute liquid mole fraction (or, alternatively, the solubility of the solute as a function of pressure). We intentionally limited the highest pressure to 90% of the mixture critical pressure, as CEOS are inherently inaccurate near the critical point. This procedure decreases the influence on the regressed interaction parameters of data in regions where the EOS is incapable of accurate predictions.

The objective function used, SS, minimizes the sum of squared-relative deviations in predicted bubble point pressures

$$\mathrm{SS} = \sum_{i}^{n} \left(\frac{p_{\mathrm{exp}} - p_{\mathrm{calc}}}{p_{\mathrm{exp}}} \right)_i^2 \tag{23}$$

where, n is the number of data points, p_{calc} the calculated pressure, and p_{exp} the experimental pressure. Detailed procedures for data reduction are given by Gasem and co-workers [4,19].

5. Parameter generalizations

Tables 3 and 4 provide definitions of five cases we evaluated, which include both the traditional and the conformal combining rules. As these tables reveal, a systematic progression in the complexity of data

Table 1
Critical properties and acentric factors used in cubic equation of state evaluations

Component	p_c (MPa)	T_c (K)	ω	Reference
Nitrogen	3.39	126.2	0.039	[26]
Hydrogen	1.30	33.2	−0.218	[26]
Carbon monoxide	3.50	132.9	0.066	[26]
Carbon dioxide	7.38	304.2	0.225	[26]
Methane	4.60	190.6	0.011	[26]
Ethane	3.87	305.3	0.100	[26]
C_3	4.25	369.8	0.153	[26]
n-C_4	3.80	425.2	0.199	[26]
n-C_5	3.37	469.7	0.251	[26]
n-C_6	3.01	507.5	0.299	[26]
n-C_7	2.74	540.3	0.349	[26]
n-C_8	2.49	568.8	0.398	[26]
n-C_9	2.29	594.6	0.445	[26]
n-C_{10}	2.13	618.8	0.489	[27]
n-C_{12}	1.83	658.9	0.575	[27]
n-C_{16}	1.39	720.9	0.737	[27]
n-C_{18}	1.23	745.5	0.814	[27]
n-C_{19}	1.16	756.6	0.851	[27]
n-C_{20}	1.09	766.9	0.888	[27]
n-C_{21}	1.03	776.6	0.925	[27]
n-C_{22}	0.97	785.7	0.961	[27]
n-C_{24}	0.87	802.3	1.031	[27]
n-C_{28}	0.71	830.3	1.167	[27]
n-C_{36}	0.48	871.5	1.421	[27]
n-C_{44}	0.34	899.8	1.656	[27]

regressions has been pursued to (a) explore the effect of variations in solute type, solvent molecular size, and temperature on EOS representations; (b) assess the correlative ability of the PR and SRK EOS; and (c) identify the optimum strategy for parameter generalization.

The summary results for the PR EOS using the new α function are given in Table 5 for all the systems as specified by Cases 1–5. Case 1, where the predictions are based solely on pure-fluid parameters, represents the raw potential of the EOS. The overall EOS accuracy for the systems considered is within 14%. In Case 2, we use *n*-paraffin-dependent C_{ij} or C_{ij} (CN). This is the commonly-used approach in most industrial applications. The results for this case show significant improvement over Case 1. This is expected since binary data are used to calibrate the EOS model. The %AAD is 3.1% for this case. In Case 4, both C_{ij} (CN) and D_{ij} (CN) are used simultaneously. Here, D_{ij} is used to account for molecular size effects, as discussed by Gasem et al. [19,28]. The quality of EOS representation improves slightly, yielding an overall AAD of 2%. Similar results are observed in Case 3, where we employ a temperature-dependent parameter, C_{ij} (CN, T). Finally, we consider Case 5, which represents the ultimate precision capability of the EOS. Two temperature-dependent parameters C_{ij} (CN, T) and D_{ij} (CN, T), are used to account for variations in solvent molecular size and temperature. The overall AAD for this case is less than about 1% for all the solutes considered. This level of representation reflects, to a large degree, the experimental imprecision.

Table 2
Binary systems database

Solvent	Temperature range (K)	Pressure range (MPa)	Solute mole fraction range	NPTS	Reference
Hydrogen					
n-C_4	327.65–394.25	2.778–16.847	0.0190–0.1930	48	[29]
n-C_5	323.15	0.347–20.680	0.0016–0.1460	11	[30]
n-C_6	344.26–411.11	1.238–24.132	0.0105–0.2150	46	[31,32]
n-C_7	424.15–498.85	2.420–8.714	0.0230–0.5370	22	[33]
n-C_{10}	344.26–423.15	3.710–17.390	0.0367–0.1288	17	[34]
n-C_{12}	344.26–410.93	1.422–123.235	0.0144–0.1252	24	[35]
n-C_{20}	323.15–423.15	2.230–12.910	0.0273–0.1289	22	[34]
n-C_{28}	348.15–423.15	2.860–13.100	0.0452–0.1572	19	[34]
n-C_{36}	373.15–423.15	3.560–16.750	0.0677–0.2271	12	[34]
Total number of points				191	
Nitrogen					
n-C_4	250.00–399.82	0.777–15.785	0.0040–0.2742	53	[36,37]
n-C_5	277.43–377.59	0.250–20.781	0.0022–0.3390	38	[38]
n-C_8	322.00–344.30	3.227–35.039	0.0430–0.3470	10	[39]
n-C_9	322.00–344.30	3.723–34.736	0.0480–0.3320	12	[39]
n-C_{10}	344.26–410.93	3.910–16.040	0.0556–0.1967	21	[40]
n-C_{12}	344.26–410.93	1.293–9.549	0.0202–0.1251	23	[35]
n-C_{20}	323.20–423.20	3.830–17.230	0.0610–0.2121	20	[40]
n-C_{28}	348.20–423.20	4.300–16.470	0.0726–0.2578	19	[40]
n-C_{36}	373.20–423.20	5.280–17.990	0.1054–0.2970	12	[40]
Total number of points				208	
Carbon monoxide					
C_3	273.15–323.15	1.379–13.790	0.0230–0.3840	20	[41]
n-C_6	323.15–423.15	1.179–8.687	0.0099–0.1466	18	[42]
n-C_8	463.15–533.15	0.669–6.569	0.0027–0.1570	42	[43]
n-C_{10}	310.93–377.59	2.227–10.004	0.0385–0.1400	17	[42]
n-C_{12}	344.26–410.93	0.690–8.751	0.0113–0.1493	27	[35]
n-C_{20}	323.15–423.15	1.991–8.384	0.0403–0.1614	20	[42]
n-C_{28}	348.15–423.15	1.903–8.412	0.0463–0.1853	26	[42,44]
n-C_{36}	373.15–423.15	1.800–8.956	0.0494–0.2099	12	[42]
Total number of points				182	
Carbon dioxide					
n-C_5	273.41	0.269–1.558	0.0451–0.3206	4	[45]
n-C_6	303.15–353.15	0.862–7.620	0.0515–0.8435	19	[46,47]
n-C_7	310.65–352.59	0.186–7.267	0.0220–0.9290	29	[48]
n-C_{10}	310.93–377.59	0.689–8.618	0.0730–0.4876	14	[49]
n-C_{16}	463.05–663.75	2.006–5.087	0.0897–0.2575	15	[50]
n-C_{18}	396.60–673.20	1.016–6.190	0.0519–0.3890	25	[51]
n-C_{19}	313.15–333.15	0.936–7.181	0.0899–0.6342	21	[52]
n-C_{20}	323.15–373.15	0.620–6.429	0.0730–0.5010	22	[19]
n-C_{21}	318.15–338.15	0.931–7.759	0.0999–0.6496	15	[52]
n-C_{22}	323.15–373.15	0.962–7.178	0.0833–0.5925	34	[53]

Table 2 (*Continued*)

Solvent	Temperature range (K)	Pressure range (MPa)	Solute mole fraction range	NPTS	Reference
n-C_{24}	373.15	1.013–5.066	0.0819–0.3531	5	[54]
n-C_{28}	348.15–423.15	0.807–9.604	0.0700–0.6170	22	[19]
n-C_{36}	373.15–423.15	0.524–5.878	0.0620–0.4590	16	[19]
n-C_{44}	373.15–423.15	0.579–6.112	0.0800–0.5020	12	[19]
Total number of points				328	
Methane					
n-C_4	277.59–377.59	1.379–10.342	0.0256–0.4513	11	[55,56]
n-C_5	344.26–377.59	1.379–13.790	0.0279–0.5320	28	[57,58]
n-C_6	298.33–373.33	1.014–10.135	0.0300–0.4125	37	[59]
n-C_7	311.11–411.11	2.193–10.466	0.1000–0.4000	12	[60]
n-C_8	298.33–423.33	1.013–7.093	0.0280–0.2870	28	[61]
n-C_9	323.15–423.15	1.014–10.135	0.0329–0.3471	39	[62]
n-C_{10}	310.93–410.93	1.043–8.647	0.0495–0.3080	32	[63]
n-C_{16}	462.45–623.15	2.029–25.260	0.0801–0.5958	15	[64]
n-C_{20}	323.15–423.15	0.953–10.690	0.0512–0.3500	22	[63]
n-C_{28}	348.15–423.15	0.926–7.092	0.0568–0.2992	18	[63]
n-C_{36}	373.15–423.15	0.838–7.928	0.0511–0.3506	13	[63]
n-C_{44}	373.15–423.15	0.677–5.572	0.0501–0.3112	15	[63]
Total number of points				270	
Ethane					
n-C_4	303.15–363.40	0.441–4.877	0.0440–0.8370	34	[65]
n-C_5	310.93–444.26	0.345–6.205	0.0048–0.8503	28	[66]
n-C_6	310.93–394.26	0.393–5.399	0.0720–0.6519	48	[67]
n-C_7	338.71–449.82	3.923–7.598	0.2960–0.8480	8	[68]
n-C_8	323.15–373.15	0.405–5.269	0.0470–0.8630	31	[69]
n-C_{10}	311.11–411.11	0.423–8.236	0.1050–0.6380	30	[70]
n-C_{16}	285.00–345.00	0.575–6.633	0.1990–0.8750	30	[71]
n-C_{20}	323.15–423.15	0.504–6.645	0.1180–0.6530	17	[72]
n-C_{24}	330.00–360.00	0.460–7.820	0.1197–0.7833	11	[73]
n-C_{28}	348.15–423.15	0.563–4.394	0.1020–0.5200	23	[72]
n-C_{36}	373.15–573.05	0.368–4.760	0.0870–0.5320	24	[72,74]
n-C_{44}	373.15–423.15	0.387–3.170	0.0986–0.5161	16	[72]
Total number of points				300	

Table 3
Case studies for cubic equation of state predictions using C_{ij} and D_{ij}

Case	Description
(1) $C_{ij} = 0$, $D_{ij} = 0$	The simple quadratic mixing rules are used, without any interaction parameters
(2) C_{ij}(CN), $D_{ij} = 0$	A single value of C_{ij} is determined for each binary system, no D_{ij} is used
(3) C_{ij}(CN, T), $D_{ij} = 0$	A separate value of C_{ij} is determined for each temperature in a system, no D_{ij} used
(4) C_{ij}(CN), D_{ij}(CN)	Both C_{ij} and D_{ij} values are determined for each system
(5) C_{ij}(CN, T), D_{ij}(CN, T)	Both C_{ij} and D_{ij} are determined for each temperature in a system

Table 4
Case studies for cubic equation of state predictions using N_{ij} and M_{ij}

Case	Description
(1) $N_{ij} = 0$, $M_{ij} = 1$	The simple quadratic mixing rules are used, without any interaction parameters
(2) N_{ij}(CN), $M_{ij} = 1$	A single value of N_{ij} is determined for each binary system, M_{ij} is set equal to 1.0
(3) N_{ij}(CN, T), $M_{ij} = 1$	A separate value of N_{ij} is determined for each temperature in a system, M_{ij} is set equal to 1.0
(4) N_{ij}(CN), M_{ij}(CN)	Both N_{ij} and M_{ij} values are determined for each system
(5) N_{ij}(CN, T), M_{ij}(CN, T)	Both N_{ij} and M_{ij} are determined for each temperature in a system

As expected, the regression results from both the conformal and the traditional combining rules are practically identical. However, for systems involving highly supercritical solutes, such as nitrogen and hydrogen, the variations in the parameter values are greater for C_{ij} than for N_{ij}, as seen in Fig. 2 for the nitrogen systems; albeit, the EOS predictions are more sensitive to variations in N_{ij} value. The optimum interaction parameters for both the traditional and conformal combining rules as specified by Cases 2–5 and their associated statistics are presented elsewhere [32].

Examination of the various cases described earlier led me to believe that Case 2 provides the best opportunity for parameter generalizations. First, using temperature-independent C_{ij} reduces the complexity of the generalized correlations with minor loss of accuracy (3% for Case 2 compared to 2% for Case 3). Second, using a single interaction parameter eliminates parameter inter-correlations that invariably exist when using multiple parameters. Third, accuracy of 3–5% is adequate in many industrial processes.

Careful evaluation of various correlation schemes for the interaction parameters indicated that acentric factor is a suitable correlating variable. Thus, the EOS parameter (N_{ij}) for each solute is correlated in terms of the solvent acentric factor, ω. Tables 6 and 7 present the generalized correlations developed in this study.

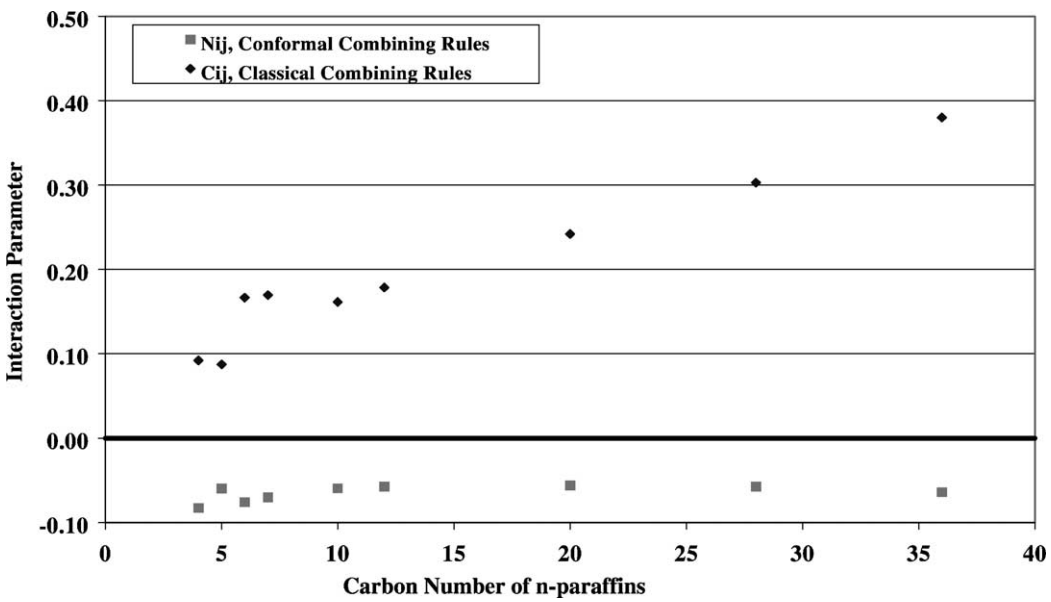

Fig. 2. Interaction parameters from classic combining rules and conformal combining rules for nitrogen + n-paraffins.

Table 5
PR equation of state representations of the bubble point pressure of the selected systems using the new α function

Case	Hydrogen		Nitrogen		Carbon dioxide		Carbon monoxide		Methane		Ethane		Overall results	
	%AAD	RMSE (bar)	%AAD	RMSE (bar)	%AAD	RMSE (bar)	%AAD	RMSE (bar)	%AAD	RMSE (bar)	%AAD	RMSE (bar)	%AAD	RMSE (bar)
(1) $N_{ij} = 0$, $M_{ij} = 1$	15.8	17.0	23.1	33.4	23.6	11.9	8.4	5.9	6.8	4.5	8.8	2.5	13.7	16.2
(2) N_{ij}(CN), $M_{ij} = 1$	2.7	3.8	3.2	4.8	4.2	2.4	3.2	2.4	2.2	2.0	3.4	1.8	3.1	3.3
(3) N_{ij}(CN, T), $M_{ij} = 1$	1.4	2.8	1.8	2.7	2.7	1.8	1.2	1.4	1.6	2.0	3.1	1.6	2.3	4.9
(4) N_{ij}(CN), M_{ij}(CN)	2.6	3.8	2.5	3.7	3.0	1.3	2.7	2.0	1.7	1.1	1.8	1.0	2.4	4.3
(5) N_{ij}(CN, T), M_{ij}(CN, T)	0.9	1.4	0.8	1.4	0.9	0.5	0.6	0.5	0.5	0.4	1.0	0.6	0.8	1.2

Table 6
PR equation of state generalized predictions of the bubble point pressure of the selected systems using both the new and original α functions: N_{ij} and M_{ij} approach

Systems	N_{ij}	M_{ij}	%AAD	RMSE (bar)	NAAD
H_2	$-0.023 - 0.015/\omega$[a]	1	3.6	4.8	1.3
	$-0.060 - 0.029/\omega$[b]	1	4.4	6.5	1.3
N_2	-0.062[a]	1	4.1	5.7	1.3
	-0.076[b]	1	3.7	4.7	1.5
CO	-0.021[a]	1	3.6	3.3	1.1
	-0.032[b]	1	3.4	3.1	1.1
CO_2	$0.042 - 0.067/\omega$[a]	1	5.3	2.5	1.2
	$0.038 - 0.066/\omega$[b]	1	5.2	2.8	1.3
CH_4	$0.017 - 0.014/\omega$[a]	1	3.0	2.0	1.4
	$0.010 - 0.014/\omega$[b]	1	3.0	2.1	1.3
C_2H_6	$0.033 - 0.020/\omega$[a]	1	4.6	2.0	1.4
	$0.034 - 0.022/\omega$[b]	1	4.8	2.0	1.5

[a] The value represents new α.
[b] The value represents original α.

Specifically, generalized-parameter correlations have been developed for the PR EOS employing both the new and original α functions (Table 6) and the original SRK EOS (Table 7). In all cases, generalized correlations for the conformal combining parameters (N_{ij}) are presented. Generalized EOS interaction parameters for the traditional combining rules (C_{ij}) may be generated from generalized N_{ij} correlations of Tables 6 and 7 and the relation provided by Eq. (21). Fig. 3 depicts the generalized correlations for the various solutes in comparison with the regressed parameters of Case 2. This figure presents only the results for the conformal combining rule using the new PR EOS α function. As illustrated, the current generalizations reproduce the trends in the regressed parameters reasonably well.

Fig. 4 presents a typical error profile for cases involving parameter regressions as well as generalized predictions. As indicated by the results shown for ethane: (a) significant errors occur, especially for CN $>$ 10, when no binary interaction parameters are used (%AAD of 35 for C_{44} in Case 1), (b) a sizeable reduction in error is realized when we account simultaneously for variations in temperature and solvent molecular size (overall %AAD of 1.0 for Case 5), (c) the error increases with increasing

Table 7
SRK equation of state generalized predictions of the bubble point pressure of the selected systems: N_{ij} and M_{ij} approach

Systems	N_{ij}	M_{ij}	%AAD	RMSE (bar)	NAAD
H_2	$-0.064 - 0.023/\omega$	1	4.8	6.4	1.6
N_2	-0.071	1	3.1	5.0	1.2
CO	-0.028	1	3.5	3.4	1.1
CO_2	$0.033 - 0.066/\omega$	1	4.8	2.6	1.1
CH_4	$0.007 - 0.011/\omega$	1	3.1	2.1	1.3
C_2H_6	$0.027 - 0.019/\omega$	1	4.8	2.0	1.4

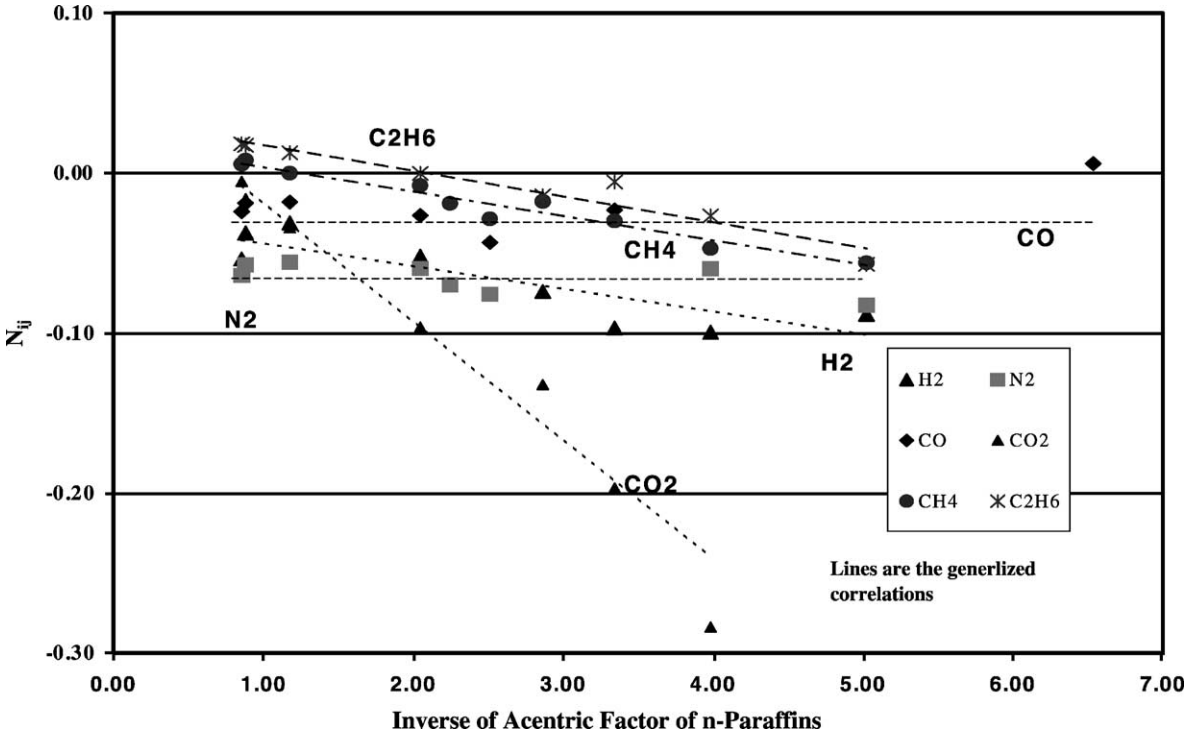

Fig. 3. Generalized parameters for asymmetric mixtures.

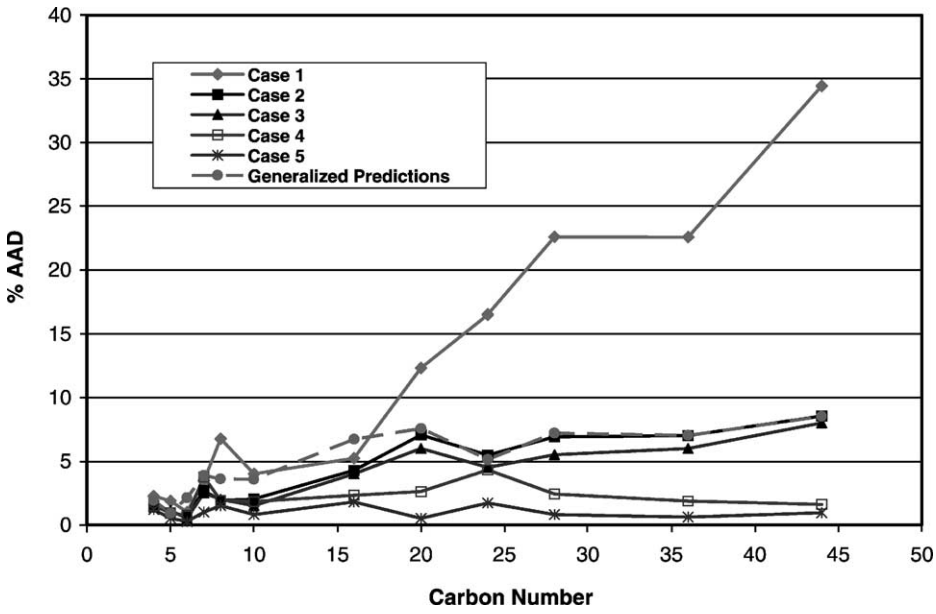

Fig. 4. PR EOS error profile for ethane parameter regressions and generalized predictions.

solvent molecular size when the co-volume correction is not considered ($D_{ij} = 0$ or $M_{ij} = 1$), and (d) the generalized predictions produce an error profile comparable to Case 2, especially for larger molecules.

The summary results in Tables 6 and 7 indicate that the generalized predictions yield AAD from 3% for methane to 5% for CO_2 (RMSE of 1–6 bar, respectively). This level of accuracy represents about 50% more error than that obtained from the corresponding correlation case (Case 2). Both the traditional and the conformal combining rules produce comparable generalization accuracy, with the "normalized" $\%AAD = [(\%AAD)_{generalization}/(\%AAD)_{regression}]$ ranging from 1.1 to 1.6.

6. Discussion

The conformal combining rule offers a useful interpretation for the numerical values of binary interaction parameters. As illustrated in Fig. 5, variation in the value of N_{ij} indicates differences in the operative combining rule. For the asymmetric mixtures considered, the regressed values of N_{ij} indicate that using the geometric-mean combining rule for 'a' is suitable, with the possible exception of CO_2. Moreover, the majority of the mixtures have small negative N_{ij} values (corresponding to positive C_{ij} values), which signifies a trend toward the Halsey–Fender combining rule. So, beyond the benefit of having a flexible combining rule, we gain some insight of how the unlike molecules are interacting. For example, previous concerns about using large values of C_{ij} ($C_{ij} > 0.2$) can be alleviated, knowing that large C_{ij} values indicate that unlike-molecule combinations are intermediate between the geometric-mean and the Halsey–Fender type combinations.

Figs. 6 and 7, respectively, present variations of the generalized N_{ij} and C_{ij} with the carbon number. The trend for the parameter variations with n-paraffin molecular size is dependent on the (a_2/a_1) or

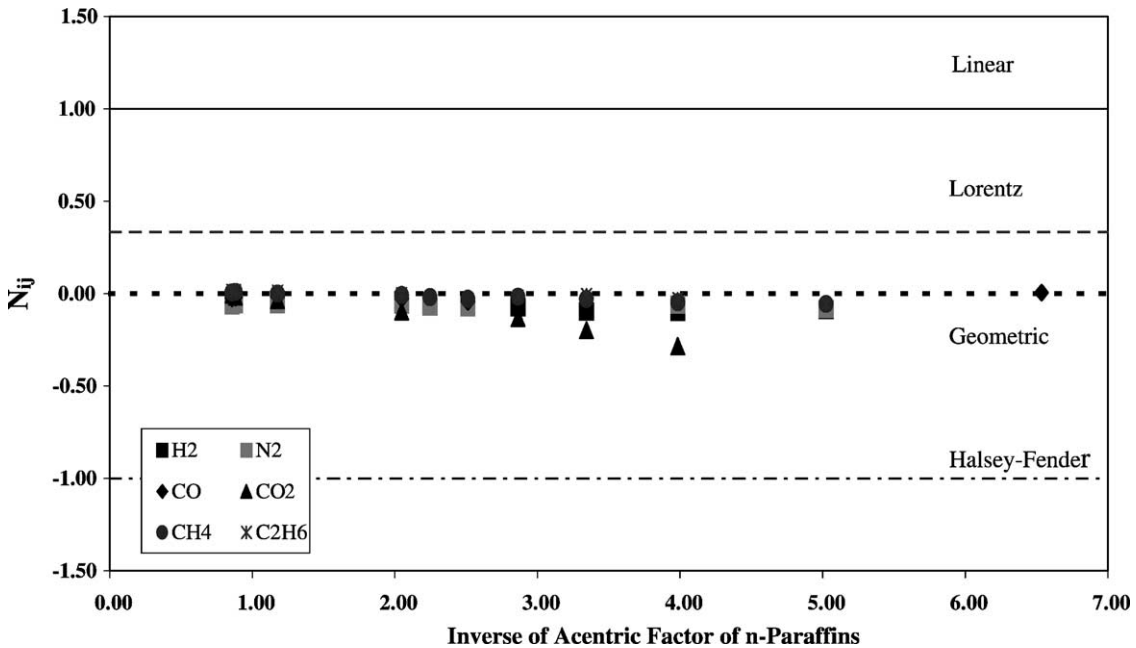

Fig. 5. Comparison of equation of state combining rules.

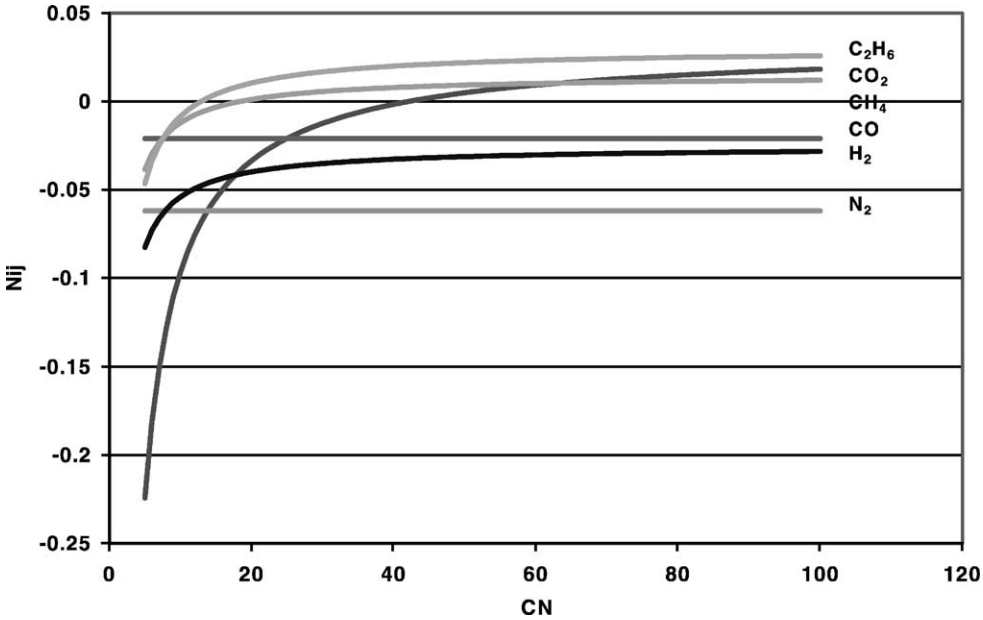

Fig. 6. PR EOS generalized conformal interaction parameters for Case 2.

($a_{\text{paraffin}}/a_{\text{solute}}$) ratio. For large ($a_2/a_1$) ratios (ratios >20), N_{ij} shows less variation than C_{ij} with molecular size, as illustrated in Fig. 6 by the nitrogen and hydrogen systems. In contrast, for lower values of (a_2/a_1) ratios (ratios <20), C_{ij} shows less variation than N_{ij} with molecular size, as illustrated by the ethane and CO_2 binaries, as shown in Fig. 7.

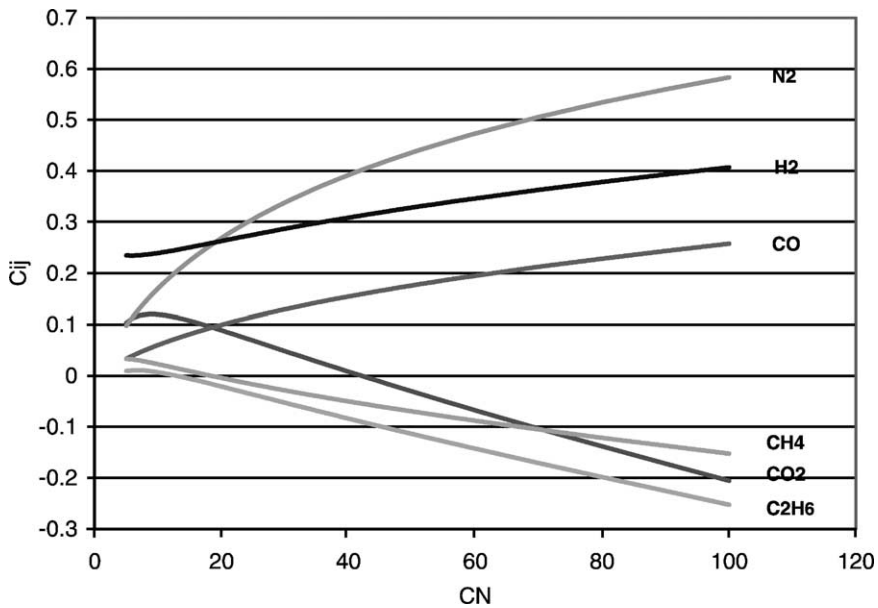

Fig. 7. PR EOS generalized traditional interaction parameters for Case 2.

The ultimate goal of our experimental studies is to develop a generalized-prediction capability for systems not measured, especially for systems involving heavy paraffins (CN > 40). Figs. 5 and 6 suggest that the conformal combining rule offers the potential for more accurate extrapolations for larger solvent molecules.

Our recent efforts to improve CEOS predictions for asymmetric mixtures have provided several useful results, including developing factors.

1. Accurate correlations for predicting the heavy *n*-paraffin critical properties and acentric factors [27].
2. Improved temperature-dependence α function for the PR EOS to predict accurately vapor pressures of heavy hydrocarbons [21].
3. An alternate EOS combining rule (present work).
4. Useful generalized-parameter correlations for two widely-used EOS (present work).
5. Group-contribution EOS generalized predictions (a forthcoming article).

More importantly, these studies have clarified several issues relating to the merits of using CEOS for asymmetric mixtures and their capability to represent such systems. First, our results clearly indicate that the accuracy of the pure-component predictions has only a moderate impact on the quality of EOS representation of mixtures involving supercritical components; that is, the advantages of having accurate vapor pressure predictions and appropriate liming behavior for the supercritical components are outweighed by the deficiencies of the mixing rules used. The nitrogen binaries provide a good example for this situation. Although our current PR EOS predicts the vapor pressures of all components accurately and the compressibility factors of nitrogen equally well (AAD of 1–2%), the a priori predictions for binary systems containing nitrogen yield over 20% average error. These results strongly suggest that additional studies are required to improve the mixing and/or combining rules for asymmetric mixtures. Second, the attractive simplicity of CEOS should not mask our need to develop theoretically-based EOS models. The desire to associate physically-meaningful interpretation to EOS model parameters is dependent on our ability to develop EOS models based on sound theory that accounts, in fundamental terms, for the molecular interactions.

7. Summary

Following the work of Juris and Wenzel, an alternate “conformal” combining rule is proposed for CEOS. The Soave–Redlich–Kwong (SRK) and Peng–Robinson (PR) EOS have been used to assess the usefulness of the alternate combining rule in describing the types of unlike interactions encountered in asymmetric mixtures. In addition, a study was undertaken to evaluate the predictive capability of both equations of state in representing vapor–liquid equilibrium of asymmetric binary mixtures, involving methane, ethane, nitrogen, hydrogen, carbon monoxide and carbon dioxide in the *n*-paraffins (C_4–C_{44}).

Although the traditional and the conformal combining rules, as expected, give identical numerical results, the conformal combining offers two distinct advantages.

1. The rule describes a wide variety of interactions between unlike molecules, as exhibited by the asymmetric mixtures considered in this study.
2. The resulting EOS interaction parameters appear to be more suitable for extrapolation; thus, generalized predictions involving heavy paraffins (CN > 40) would be more reliable.

EOS binary interaction parameters generated by the proposed combination rule are presented for the systems considered. The quality of the EOS representation is dependent on the level of complexity applied in the parameter regressions. Overall, AAD of 1–3% are realized from the various regression scenarios.

In addition, generalized EOS parameter correlations for system-dependent parameters have been developed. These interaction parameters represent the solubilities of the selected systems within 5%.

List of symbols

a, b	equation of state parameters
%AAD	average absolute percent deviation
CN	carbon number
C_{ij}, D_{ij}	interaction parameters
k	intermediate function in equation of state
MW	molecular mass
n	number of components
N_{ij}, M_{ij}	exponents of the conformal combing rule
NAAD	normalized average absolute deviations; $(\%AAD)_{generalization}/(\%AAD)_{regression}$
NPTS	number of data points
p	pressure
R	universal gas constant
RMSE	root mean square error
SS	objective function
T	temperature
v	specific volume
z	mole fraction

Greek letters

α	equation of state temperature dependence function
ω	centric factor

Subscripts and superscripts

c	critical state
calc	calculated
exp	experimental
r	reduced property

References

[1] K. Juris, L.A. Wenzel, AIChE Symp. Series 70 (1974) 70–79.
[2] G. Soave, Chem. Eng. Sci. 27 (1972) 1197–1203.
[3] D.Y. Peng, D.B. Robinson, Ind. Eng. Chem. Fundam. 15 (1976) 59–64.
[4] K.A.M. Gasem, C.H. Ross, R.L. Robinson Jr., Can. J. Chem. Eng. 71 (1993) 805–816.
[5] C-H. Kim, P. Vimalchand, M.D. Donohue, S.I. Sandler, AIChE J. 30 (1986) 1726–1735.
[6] R.D. Shaver, R.L. Robinson Jr., K.A.M. Gasem, Fluid Phase Equilib. 112 (1995) 223–248.
[7] W.G. Chapman, K.E. Gubbins, G. Jackson, M. Radosz, Ind. Eng. Chem. Res. 29 (1990) 1709–1721.
[8] K.H. Row, Ph.D. Dissertation, Oklahoma State University, Stillwater, OK 1998.

[9] A.G. Mansoori, Fluid Phase Equilib. 87 (1993) 1–22.
[10] S.K. Shibata, S.I. Sandler, Ind. Eng. Chem. Res. 28 (1989) 1893–1898.
[11] P.T. Eubank, G.S. Shyu, N.S.M. Hanif, Ind. Eng. Chem. Res. 34 (1995) 314–323.
[12] H. Orbey, S.I. Sandler, AIChE J. 41 (1995) 683–690.
[13] C.H. Twu, J.E. Coon, J.R. Cunnungham, Fluid Phase Equilib. 105 (1995) 49–61.
[14] N. Trivedi, M.S. Thesis, Oklahoma State University, Stillwater, OK, 1996.
[15] J.F. Luongo-Ortiz, K.E. Starling, Fluid Phase Equilib. 132 (1997) 159–167.
[16] A. Kordas, K. Tsoutsouras, S. Stamataki, D. Tassios, Fluid Phase Equilib. 93 (1994) 141–166.
[17] A. Kordas, K. Magoulas, S. Stamataki, D. Tassios, Fluid Phase Equilib. 112 (1995) 33–44.
[18] H. Nishiumi, T. Arai, K. Takeuchi, Fluid Phase Equilib. 42 (1988) 43–62.
[19] K.A.M. Gasem, Ph.D. Dissertation, Oklahoma State University, Stillwater, OK, 1986.
[20] J. Tong, M.S. Thesis, Oklahoma State University, Stillwater, OK, 1994.
[21] W. Gao, K.A.M. Gasem, R.L. Robinson Jr., Fluid Phase Equilib., 2000.
[22] A.Z. Panagiotopoulos, R.C. Reid, Fluid Phase Equilib. 29 (1986) 525–534.
[23] V.I. Harismiadis, A.Z. Panagiotopoulos, D.P. Tassios, Fluid Phase Equilib. 94 (1994) 1–18.
[24] M. Sudibandriyo, M.S. Thesis, Oklahoma State University, Stillwater, OK, 1991.
[25] K.A.M. Gasem, B.A. Bufkin, A.M. Raff, R.L. Robinson Jr., J. Chem. Eng. Data 34 (1989) 187–191.
[26] R.C. Reid, J.M. Prausnitz, B.E. Poling, The Properties of Gases and Liquids, fourth ed., McGraw-Hill, New York, 1987.
[27] W. Gao, K.A.M. Gasem, R.L. Robinson Jr., Fluid Phase Equilib. 179 (2001) 207–216.
[28] K.A.M. Gasem, R.L. Robinson Jr., J. Chem. Eng. Data 30 (1985) 53–56.
[29] A.E. Klink, H.Y. Cheh, E.H. Amick Jr., AIChE J. 21 (1975) 1142–1148.
[30] N.P. Freitag, D.B. Robinson, Fluid Phase Equilib. 31 (1986) 183–201.
[31] W.B. Nichols, H.H. Reamer, B.H. Sage, AIChE J. 3 (1957) 262–267.
[32] W. Gao, Ph.D. Dissertation, Oklahoma State University, Stillwater, OK 1999.
[33] S. Peter, K. Reinhartz, Zeit. Fur. Phys. Chem. 24 (1960) 103–119.
[34] J. Park, R.L. Robinson Jr., K.A.M. Gasem, J. Chem. Eng. Data 40 (1995) 241–245.
[35] W. Gao, K.A.M. Gasem, R.L. Robinson Jr., J. Chem. Eng. Data 44 (1999) 185–189.
[36] T.S. Brown, V.G. Niesen, E.D. Sloan, A.J. Kidnay, Fluid Phase Equilib. 53 (1989) 7–14.
[37] W.W. Akers, L.L. Attwell, J.A. Robinson, Ind. Eng. Chem. 46 (1954) 2539–2540.
[38] H. Kalra, D.B. Robinson, G.J. Besserer, J. Chem. Eng. Data 22 (1977) 215–218.
[39] F.M. Llave, T.H. Chung, J. Chem. Eng. Data 33 (1988) 123–128.
[40] J. Tong, W. Gao, K.A.M. Gasem, R.L. Robinson Jr., J. Chem. Eng. Data 44 (1999) 784–787.
[41] D.B. Trust, F. Kurata, AIChE J. 17 (1971) 415–419.
[42] X. Yi, M.S. Thesis, Oklahoma State University, Stillwater, OK, 1992.
[43] J.F. Connolly, G.A. Kandalic, J. Chem. Thermodyn. 16 (1984) 1129–1139.
[44] S. Srivatsan, M.S. Thesis, Oklahoma State University, Stillwater, OK, 1991.
[45] H. Cheng, M.E. Fernandez, J.A. Zollweg, W.B. Streett, J. Chem. Eng. Data 34 (1989) 319–323.
[46] K. Ohgaki, T. Katayama, J. Chem. Eng. Data 21 (1976) 53–55.
[47] Z. Wagner, I. Wichterle, Fluid Phase Equilib. 33 (1987) 109–123.
[48] H. Kalra, H. Kubota, D.B. Robinson, H. Ng, J. Chem. Eng. Data 23 (1978) 317–321.
[49] H.H. Reamer, B.H. Sage, J. Chem. Eng. Data 8 (1963) 508–513.
[50] H.M. Sebastian, J.J. Simnick, H. Lin, K.C. Chao, J. Chem. Eng. Data 25 (1980) 138–140.
[51] H. Kim, H. Lin, K.C. Chao, AIChE Symp. Ser. 81 (1985) 96–101.
[52] D.J. Fall, J.L. Fall, K.D. Luks, J. Chem. Eng. Data 30 (1985) 82–88.
[53] D.J. Fall, J.L. Fall, K.D. Luks, J. Chem. Eng. Data 29 (1984) 413–417.
[54] F. Tsai, J. Yau, J. Chem. Eng. Data 35 (1990) 43–45.
[55] H.C. Wiese, J. Jacobs, B.H. Sage, J. Chem. Eng. Data 15 (1970) 82–91.
[56] L.R. Roberts, R.H. Wang, A. Azarnoosh, J.J. McKetta, J. Chem. Eng. Data 7 (1962) 484–485.
[57] N.W. Prodany, B. Williams, J. Chem. Eng. Data 16 (1971) 1–6.
[58] H.S. Taylor, G.W. Wald, B.H. Sage, W.N. Lacey, Oil Gas J. 38 (1939) 46–49.
[59] J. Shim, J.P. Kohn, J. Chem. Eng. Data 7 (1962) 3–8.
[60] H.H. Reamer, B.H. Sage, W.N. Lacey, Chem. Eng. Data Ser. 1 (1956) 29–42.

[61] J.P. Kohn, W.F. Bradish, J. Chem. Eng. Data 9 (1964) 5–8.
[62] L.M. Shipman, J.P. Kohn, J. Chem. Eng. Data 11 (1966) 176–180.
[63] N.A. Darwish, J. Fathikalajahi, K.A.M. Gasem, R.L. Robinson Jr., J. Chem. Eng. Data 38 (1993) 44–48.
[64] H.M. Lin, H.M. Sebastian, K.C. Chao, J. Chem. Eng. Data 25 (1980) 252–254.
[65] V. Lhotak, I. Wichterle, Fluid Phase Equilib. 6 (1981) 229–235.
[66] H.H. Reamer, B.H. Sage, W.N. Lacey, J. Chem. Eng. Data 5 (1960) 44–50.
[67] K.A.M. Gasem, A.M. Raff, N. Darwish, R.L. Robinson Jr., J. Chem. Eng. Data 34 (1989) 397.
[68] V.S. Mehra, G. Thodos, J. Chem. Eng. Data 10 (1965) 211–214.
[69] A.B.J. Rodrigues, D.S. McCaffrey Jr., J.P. Kohn, J. Chem. Eng. Data 13 (1968) 164–168.
[70] B.A. Bufkin, R.L. Robinson Jr., S.S. Estera, K.D. Luks, J. Chem. Eng. Data 31 (1986) 421–423.
[71] R. Goede, C.J. Peters, H.J.V.D. Kooi, R.N. Lichtenthaler, Fluid Phase Equilib. 50 (1989) 305–314.
[72] K.A.M. Gasem, A.M. Raff, B.A. Bufkin, R.L. Robinson Jr., J. Chem. Eng. Data 34 (1989) 187–191.
[73] C.J. Peters, V.D.H.J. Kooi, D.S.J. Arons, J. Chem. Thermodyn. 19 (1987) 395–405.
[74] F. Tsai, S.H. Huang, H. Lin, K.C. Chao, J. Chem. Eng. Data 32 (1987) 467–469.